Report on Radar Coverage and Propagation Conditions in the area of Chicago O'Hare International Airport, Nov 7, 2006

Martin Shough
NARCAP Research Associate

Adapted from *Section 6* of

Report of an Unidentified Aerial Phenomenon and its Safety Implications at O'Hare International Airport on November 7, 2006Case 18

http://www.narcap.org/reports/010/TR10_Case_18a.pdf

By
Richard F. Haines, Ph.D. Senior Editor
Chief Scientist
with
K. Efishoff, D. Ledger, L. Lemke, S. Maranto, W. Puckett,
T. Roe, M. Shough, R. Uriarte

March 9, 2007

http://www.NARCAP.org

National Aviation Reporting Center on Anomalous Phenomena

Report on Radar Coverage and Propagation Conditions

Martin Shough*
March 2007

1. Abstract

Visual reports of an unidentified aerial phenomenon rising through a 1900' overcast at Chicago O'Hare International Airport on Nov 7 2006 raise the prospect of radar detection by FAA surveillance radars. Pending acquisition of radar tape data[1] by NARCAP the present report addresses:

- available technical specifications of ATC and joint-use defence surveillance radar heads covering the relevant C-90 control area

- the roles of these radars in the FAA National Airspace System architecture

- the siting of the several radar heads and their coverage volumes

- results from NWS Doppler weather radar coverage of the sighting location

- radar propagation conditions at the time of the reported observations

- preliminary conclusions on factors likely to affect interpretation of possible radar data

---

1 Raw ATC radar data were recovered from FAA and examined, as detailed in the complete NARCAP report. No clearly relevant detections were discovered. Weather radar echo is discussed in Sections 4 & 6 of the present document.

2. Radar system types and characteristics

Air surveillance radars

ASR-9 (Airport Surveillance Radar Model 9; Northrop Grumman)

The radars of principal interest in this study. FAA Terminal Radar Approach Control (TRACON) radars operating in primary and SSR modes, responsible for TRACON surveillance volume designated C-90, surface to 13,000 ft within 40 mile radius of O'Hare (KORD), remote cable feeds to central TRACON facility at Elgin, Ill., 30 miles NW of O'Hare. ASR-9 also has weather data channel, optionally integrating 6-level precipitation reflectivity data onto display with refresh rate of 30 seconds (a Weather Systems Processor upgrade has been made to some ASR-9s adding doppler wind velocities and an improved update rate).

Frequency	S-Band, 2.7-2.9 GHz (~10 cm)
Polarisation	Linear or r/h circular
Peak power	1.1 MW
Pulse width	1.08 microsec
PRF	928 & 1193 pps
	1027 & 1321pps
Range performance	$1m^2$ @ 111 km (60 nmi)
Elevation beamwidth	4.8 Degrees
Az Beamwidth	1.4 Degrees
Beam shaping	Cosecant [2]
Rotation rate	12.5 RPM (4.8 sec)

Table 1. ASR-9 specifications

This radar has a dual horn parabolica antenna producing two beams, utilising the same frequency but with different vertical profiles, giving high and low beams. The receiver toggles sequentially between the two patterns, which improves signal detectability at

shorter ranges by minimising clutter (coverage is discussed in *Section 4* below). The Plan Position Indicator (PPI) display has operator-selectable range scales to a maximum 60 nmi scale.

The signal receiver/processor applies Sensitivity-Time Control (STC) swept video gain to the display product (suppressing echo strengths at shorter ranges to even out PPI brightness and improve subclutter visibility) and also uses Moving Target Detection (MTD) in its Doppler filtering software to further suppress ground clutter and enhance visibility of moving targets.

The ASR-9 divides its 60 nmi range domain into 960 annuli of 1/16 nmi (~375 ft) range depth, and each annulus into 256 azimuth cells of ~ 1.4 degs. Each azimuth cell (the dwell time of a point target in one beamwidth) is filled with 18 pulses, divided into two pulse repetition intervals of 10 pulses at a higher PRF followed by 8 pulses at a lower, which allows signal processing software to improve target detection and eliminate certain problems (see *Section 6*). Returned pulse echoes are assigned in batches to their appropriate range cell to be analysed by sets of 10 and 8 phase detectors respectively, which measure pulse-to-pulse changes in Doppler frequencies. The results for each cell are integrated and measured against a reactively adjusted noise threshold (CFAR or Constant false Alarm Rate filter) which allows the processor to decide whether or not a target is present.

It can be seen that the cell size represents a limit of discrimination on the PPI defined by beam width and pulse length (actually 1/2 pulse length). It is not possible to determine the position of a target to a precision finer than the range and azimuth dimensions of the cell, or to resolve two targets physically closer than the dimensions of the cell. A similar "resolution cell" is a limitation of all types of surveillance radars.

ARSR-3 (Air Route Surveillance Radar Model 3; Westinghouse)

Joint-use FAA and military. Long range (~200 nmi) primary surveillance radars for en route ATC, operating with ATCBI-5/6 beacon interrogators for transponder traffic, remote feed to central ARTCC facility (ZAU) at Aurora, Ill.

This is a dual channel radar with two separate transmitter, receiver and signal-processing channels utilising adjacent frequencies. A minimum frequency separation of 25 MHz and orthogonal polarisation prevents co-interference. This frequency-diversity reduces signal degradation effects and improves S/N for long range targets. It also allows improved high-elevation short-range cover by using a low beam for long range low altitude cover and a slightly higher beam which minimises clutter at short ranges. Digital signal processing techniques include sliding window, Moving Target Indicator (MTI), Constant False Alarm Rate(CFAR), Range Azimuth Gating (RAG), and Sensitivity-Time Control (STC, or "swept gain"). Polarization diversity allows weather and target information to be displayed simultaneously.

The FAA National Airspace System architecture (*ref 12*) describes the ARSR-3 as follows:

The Air Route Surveillance Radar Model 3 (ARSR-3) is a 1980s radar that provides primary long-range surveillance data, including slant range and azimuth data. It processes the returns which includes demodulation, analog-to-digital conversion, moving target indicator (MTI) function, sensitivity time control, range and azimuth gating, and digital target extraction - all of which are performed digitally (with the exception of the demodulation and analog-to-digital conversion). In addition, the ARSR-3 has a weather channel with associated processing to provide weather contour information in digital format

Frequency	L-band, dual channel (1.25-1.35 GHz)
Polarization	Linear or circular
Peak power	5 MW
Average power	3.5 kW
Pulse width	2 microsec
PRF	310-365 pps
Range	200 nmi: duplex 2m^2 @ 240 nmi simplex 2m^2 @ 193 nmi
Height cover	60,000 ft
Elevation beamwidth	+3.6 to +44 degrees +2 to +42 degrees
Az beamwidth	1.1 degree
Beam shaping	cosecant ^{2}
Range resolution	0.25 nmi
Rotation rate	5 rpm (12 sec)

Table 2. ARSR-3 specifications

ARSR-4 (Air Route/Reconnaissance Surveillance Radar Model 4; Northrop Grumman)

Joint-use, military and FAA, primarily air defence, longer range (~250 nmi) primary surveillance radar installed as part of FAA/Air Force Radar Replacement (FARR) upgrade of ARSR-3 radar for perimeter defence and first-contact coastal air traffic control of CONUS up to100,000 ft altitude.

Frequency	L-band, 1.215 -1.400 GHz (~30cm) dual channel, frequency hopping
Polarisation	linear or circular
Peak power	60 kW
Range	250 nmi in duplex mode
Pulse width	150 microsec
Height cover	100,000 ft
Az beamwidth	1.4 deg
Elevation beamwidth	-7 deg to +30 deg stacked beam phased array 9 x >2 deg beams
Elevation resolution	2 deg
Rotation rate	5 rpm (12 sec)

Table 3. ARSR-4 specifications

ARSR-4 is a 3D radar producing slant range, azimuth and height data. Its electronics are all solid state for high reliability, low maintenance, having a phased array antenna that produces nine stacked beams, reducing in vertical resolution with increasing elevation. The lowest beam will tend to detect the most distant targets and hence has the finest elevation resolution (~2 degrees). Jamming and interference are suppressed by dual-channel frequency hopping (minimum channel separation 83 MHz) and by an antenna design producing low-gain sidelobes. Pulse length is on the order of 100 times that of ASR-9 and ARSR-3 radars, which allows a useful average power to be attained using much lower peak power.

Range resolution is (presumably) preserved by using digital pulse compressiotechniques. However this does not rescue the radar from a severe minimum range limitation imposed by the uncompressed pulse length. In normal long range surveillance mode this is not an operational concern however.

Weather radars

TDWR (Raytheon)

Terminal Doppler Weather Radars, multiple heads sited at Chicago O'Hare and Chicago Midway, producing multi-level digital surveillance and doppler precipitation and winds data at ~ 150m - 300m range resolution and <1 degree cross-range resolution (pencil beam) to ~ 250 miles range. Sited to detect wind shear, gust and microburst hazards along approach paths. TDWR uses a complex scan algorithm including a low-elevation scan mode with a one-minute total update rate in a high-resolution 5 nmi window around airport.

Frequency C-band	5.5 - 5.65 GHz
Polarization	Linear
Peak Power	250 KW
Pulse Width	1.1 microsec
PRF	2000 (max)
Receiver Sensitivity	0 dBz @ 190 km $1\ m^2$ @ 460 km
Elevation Beamwidth	0.55 Degrees (min)
Az Beamwidth	0.55 Degrees

Table 4. TDWR specifications

NEXRAD (Next Generation Weather Radar)

WSR-88D weather radars, multiple overlapping coverage with doppler resolution to 124 nmi and reflectivity to 248 nmi. Doppler resolution comparable to TDWR, reflectivity resolution approx 1 km data blocks. Complete volume scan update rate depends on mode of operation: over 10 mins in clear air mode; 5 - 6 mins in weather mode.

Frequency	S-band, 2.7 to 3.0 GHz
Peak power	750 kW
Average power	1.56 kW
Pulse widths	1.6 & 4.5 - 5.0 microsec
PRF	318 - 382 pps 318 - 1304 pps
Antenna	9m (18 ft) parabolic
Beamwidth	0.99 deg
Polarisation	Linear horizontal
Sidelobes	-27 dB
Point target detection	4 cm² @ 100 km
Update rate	clear air mode >10 mins weather mode >5 minutes

Table 5. WSR-88D specifications

TDWR and NEXRAD data are integrated with the ASR-9 picture into the Integrated Terminal Weather System (ITWS) product displayed at Elgin TRACON. Chicago O'Hare ATC Tower is believed not to have access to full ITWS product but may have partial data (relies on forecast and updates from ARTCC meteorogical centre, Aurora).

surface surveillance radar

ASDE-3

The ASDE-3 (Airfield Surface Detection Equipment) is a ground-scanning radar designed for managing planes, people and ground traffic on the runways and taxiways, detecting obstructions and predicting collision hazards in conjunction with Airfield Movement and Safety Systems (AMASS) software. Also used for perimeter security.

The ASDE-3 is a very short wavelength (millimeter) radar with 40 ns pulse giving very fine range resolution and a narrow (0.25 deg) azimuth beam width scanning the airport ground environment at 60 RPM. Display product in Air Traffic Control tower. Capable of detecting individual persons on the airfield.

3. Antenna Sites

Air surveillance radar sites

ASR-9, ORD #1

The main FAA surveillance radar serving Chicago O'Hare is designated in the FAA NAS Architecture (*ref.12*) as CHICAGO SRR (ORD) located in Dupage County, Illinois. Most of O'Hare Airport is located in Cook County. However satellite photos (*Fig.1*) show what appears to be anASR-9 radar antenna tower on the west side of the airfield, 600m over the county border inside Dupage County, consistent with the statement of a case witness and with the FAA information.

Fig.1 ASR-9, ORD #1, Chicago O'Hare, Dupage County, Ill.

It is possible that the second tower shown here to the north of the ASR-9 was for the now-disused ASR-7, retained in use temporarily as back-up until the relocation of ATC facilities to the new TRACON at Elgin, Illinois, too remote for effective data transmission from the ASR-7.

ASR-9, ORD #3

Most references describe (and lament) a single ASR-9 radar source but mention also a second back-up radar. A US Dept. of Transportation Report (*ref.1*) refers to:

> Limited coverage of their two ASR-9 radars, mentioned attempts to get
> radar coverage to achieve 3 nm separations within 40 nm. The TRACON
> operates 2 ASR 9's with different coverage.
> The QXM radar does not cover the NE and NW cornerposts and when
> they use it, it affects the operations. Had upgrades over the
> summer but winters have been tough with radar outages. They have
> lost their ASR 7 and then must use QXM as the backup.

The ASR-7 referred to is apparently the older analogue radar previously used as a back-up and removed a few years ago, shifting the burden onto QXM as regular back-up. Press references locate the second back-up ASR-9 radar at South Tinley Park, about 25

Fig.2. ASR-9, ORD #3, Oak Forest, Cook County, Ill.

miles SSW of O'Hare. One source also indicates that this radar normally serves Chicago Midway, which airport was for this reason unaffected by recent downtime of the O'Hare radar. A National Transportation Safety Board report (*ref. 2*), identifies

> the ASR-9 (QXM) radar antenna that is located at latitude/longitude N41-37-17.38 / W087-46-10.12, elevation 669.7 feet, magnetic variation 2 degrees west. The radar antenna supplies data to an Automated Radar Terminal System (ARTS) IIIA at C90.

These coordinates locate the antenna shown in Fig.2 near the district of Oak Forest, Cook County, a couple of miles from Tinley Park and about 11 miles south of Chicago Midway Airport, confirming the identification of this site as the one designated in the FAA National Airspace System Architecture as CHICAGO-OAK FOREST (ORD #3) SRR [QXM].

(Note: Oddly, given the established designation of Oak Forest as ORD #3, CHICAGO SRR ORD #2, Cook County, does not yet exist but according to the FAA NAS architecture is scheduled for installation in 2009.)
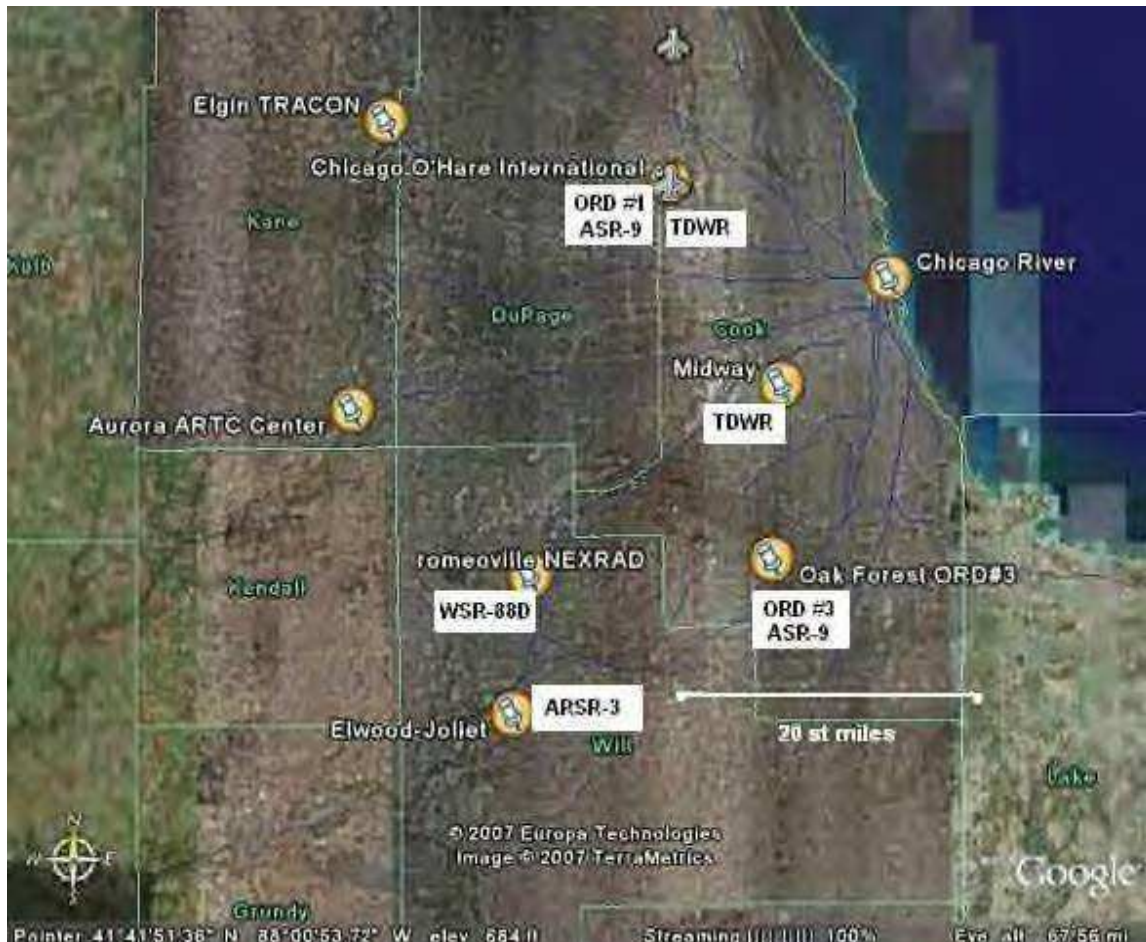

Fig.3. Locations of Chicago area radars

ARSR-3

The FAA NAS Architecture locates this long-range en route radar at ELWOOD-JOLIET (JOL) approximately as shown in Fig.3, but the antenna has yet to be identified.

ARSR-4

Nearest ARSR-4 site is at Empire, north Lake Michigan [QJA]. Fig.4 shows the position of this long-range radar in relation to the Chicago area. The exact antenna location remains uncertain.
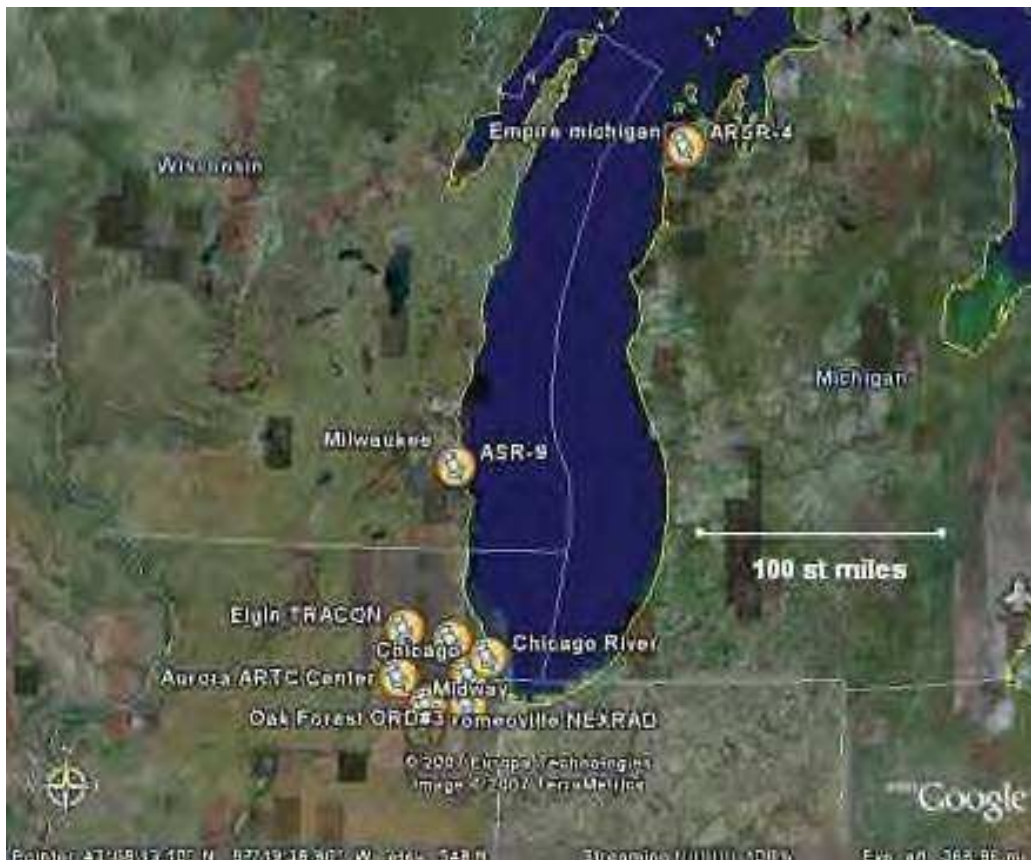

Fig.4. Radar locations around Lake Michigan.
Showing the ARSR-4 at Empire, Michigan, and ASR-9 at Milwaukee.
The maximum range of the latter falls a few miles short of the area of
the incident at Chicago O'Hare.

Weather radar sites

TDWR

TDWR weather radars are sited at both Chicago O'Hare and Chicago Midway airports. Exact antenna siting unknown. See S*ection 4*.

NEXRAD

The nearest NEXRAD WSR-88D radar is at Romeoville, Illinois (*Fig.5*). See *Section 4*.

Fig.5 NEXRAD WSR-88D weather radar at Romeoville, Ill.

Surface surveillance radar site

ASDE-3

The ASDE-3 antenna is located in a radome atop the new 250 ft Air Traffic Control Tower at the south corner of the main Chicago O'Hare terminal building complex.

4. Radar coverages

Air surveillance radars

Surveillance radar coverage is a toroidal volume centered on the antenna. A radar horizon occurs beyond which targets at low altitude may not be detected due to the curvature of the earth. The distance to the radar horizon is generally about 15% greater than the distance to the visual horizon because microwaves, unlike visible light, are significantly refracted by the standard atmosphere. Locally, the distance to the horizon may be modified by intervening hills and other diffraction obstacles, as well as by propagation conditions.

Some crude range and horizon information for these ASR and ARSR radars is summarised in *Table 6*. The maximim ranges are nominal, horizon ranges are calculated using standard refractivity assumptions (but see *Section 5*) and calculated antenna heights.

Shadow measurements on satellite photographs (see *Figs. 1 & 2*) were used to estimate antenna tower heights. The sun elevation angle is not known *a priori*, but shadows of nearby structures of relatively well-known scale were used to calibrate these measurements, which, given the uncertainty and the small difference, might reasonably be regarded as error brackets on a common tower height in the order of 100 ft. Tower heights were then added to local heights MSL to give true antenna heights relative to the sighting location.

radar type/location	max range (n.miles)	range from O'Hare C17	antenna ht (ft AGL)	horizon ranges (n.mi) at		
				1 kft AGL	2 kft AGL	3 kft AGL
ASR-9 (ORD #1) / O'Hare	60	0.78	130	52	69	81
ASR-9 (OED #2) / unknown	60	unknown	n/a	n/a	n/a	n/a
ASR-9 (ORD #3) / Oak Forest	60	22	90	52.5	68.6	80.9
ARSR-3 / Joliot-Elwood	200	35	unknown	n/a	n/a	n/a
ARSR-4 / Empire	250	210	unknown	n/a	n/a	n/a

Table 6. Sample range and horizon figures for Chicago area surveillance radars

In the case of ORD #1, sited at O'Hare, measurements AGL of antenna height and target height use a common datum point and there is no significant variation. Variation in local

topography could be potentially significant for ORD #3 however. This was investigated by taking spot height measurements at approximate 1.47 nmi (1.7 st. mi) intervals along the line of sight between Oak Forest and Chicago O'Hare as shown in *Fig.6*.
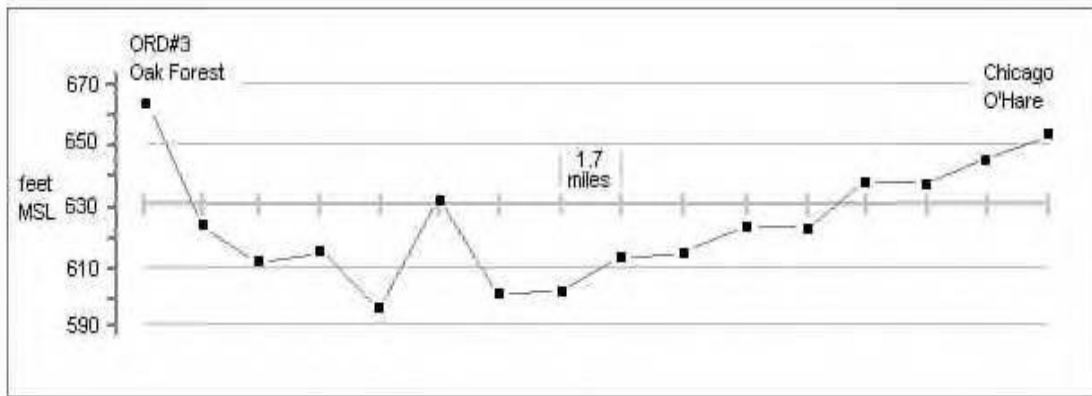

Fig.6 Topographic profile on line of sight between ORD #3 and sighting location

We find that ORD #3 is sited some 10 ft MSL higher than O'Hare (tending only to cancel part of a possible difference in tower height) and that there is no evidence of significant diffraction obstacles in the line of sight. The terrain can be considered to be a fairly uniform flat reflector and coverage will be quite well represented by the theoretical curves (assuming standard propagation; see *Section 5*).

The ASR-9 coverage pattern was then investigated in more detail. A vertical polar diagram of an ASR-9 radiation pattern is shown in *Fig. 7*. Range performance is measured in terms of probability of detection (P_d) of a target of a given cross-section, and maximum usable range is defined by a P_d = 0.8 or greater. The two curves in *Fig.7* represent contours of equiprobability of detection for a target of $1m^2$ in each of the two beams. The ASR-9 low beam is optimised for low elevation targets (peak sensitivity at ~2.5 degs) at longer ranges generally beyond 15 - 20 nmi out to the maximum range of 60 nmi; the high beam (peak sensitivity at ~7 degs) is optimised for subclutter visibility of shorter range targets at higher elevations.

These curves probably average-over some lobing detail at low elevations, especially in the case of the low beam, but can be interpreted to mean that a target of $1m^2$ radar cross-section at a couple of thousand feet altitude 22 nautical miles from ORD #3 (i.e., above Chicago O'Hare Concourse C) would return a detectable signal with a P_d = 0.8 or greater in both of the alternating beams.
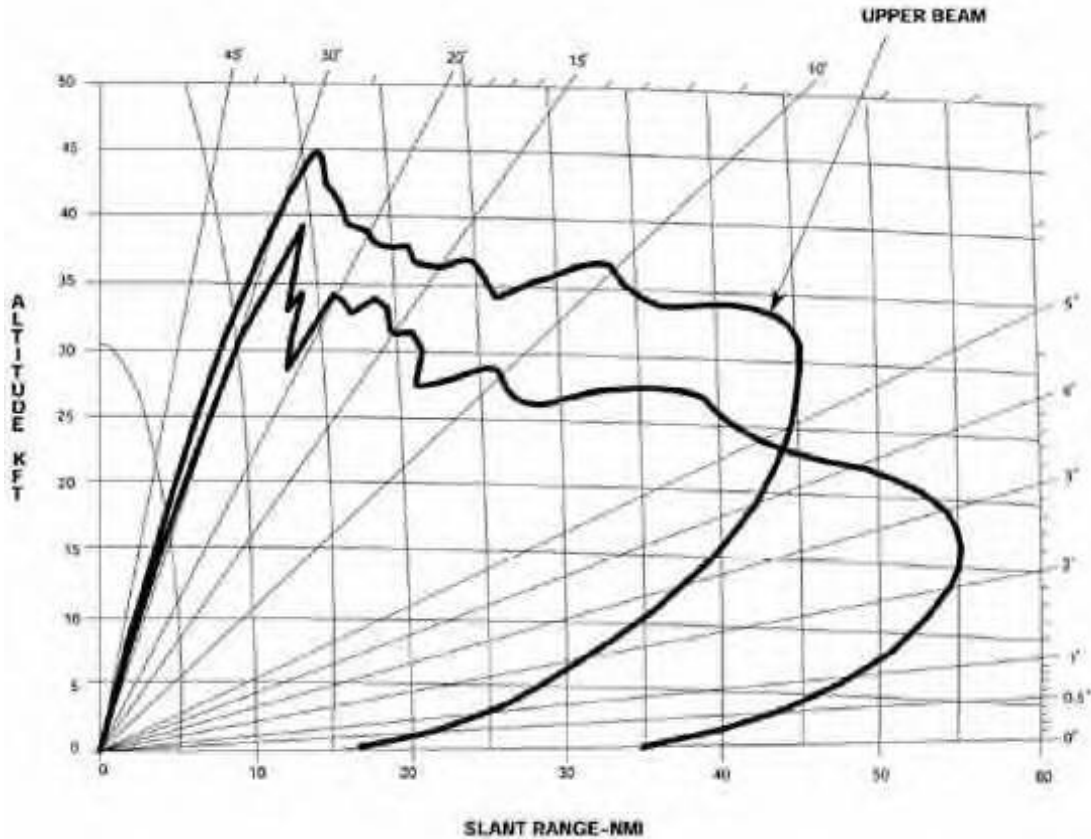
Fig.7. ASR-9 radiation pattern VPD
showing contours of equiprobability of detection for a 1m² target in
high and low beams
(from ref. 3)

The ORD #1 ASR-9 antenna at Chicago O'Hare is only about 0.8 nmi from the sighting location above Concourse C. The short range is not in a limitation in principle (disregarding here PPI range scale, STC video gain, and other operational issues discussed in *Section 6*), since the short 1.08 microsec pulse of the ASR-9 permits a minimum range (half pulse length) as small as about 150 m. The elevation of a target close to the cloud base above Concourse C would be about 18 degs, at which elevation the ASR-9 low and high beams should detect a 1m² target to slant ranges of around 17 and 20 nmi respectively. High beam returns would be favoured, with a sensitivity 16% better than the low beam and enhanced subclutter visibility at the display.

The JOLIET-ELWOOD ARSR-3 is around 35 nmi from the target area. No detailed topographic survey of the line of sight was made since neither the location nor the antenna height are known with accuracy. But the area is generally quite flat, with height variations only in the order of +/- 100ft at most and one would expect the horizon ranges to be similar to those given for the ASR-9s in *Table 6*. A target at or below the cloud base at O'Hare would generally speaking be above the radar horizon out to a range of about 64

nmi (given standard refractivity) or almost twice the distance to the sighting location.

The ARSR-4 at Empire, Michigan, is 210 nmi from the sighting location, which therefore falls inside the nominal maximum slant range of 250. But at 210 nmi range the radar horizon in normal propagation conditions will be around 26,000 ft

weather radars

TDWR

The coverage and refresh rate of the TDWR at O'Hare are uncertain, depending on siting and operational choices. The surveillance strategy is either:

> *a*) narrow sector scans aligned on approach paths (the strategy favoured for early TDWR installations) in which case there would no coverage of the region above Concourse C, or

> *b*) 360 deg complete volume scans of 5-6 minutes duration (a strategy often adopted later, saving wear on turning gear) incorporating automatic scan mode changes in response to hazard detections. In this volume scan mode TDWR can incorporate a low-elevation scan with one-minute update rate in a high-resolution 5nm window around airport, with automatic changes of scan mode in response to hazard detections.

At O'Hare (*b*) is considered more likely because of the number of runways on divergent headings, making dedicated sector-scanning of approach and departure paths uneconomical and inefficient. In this case the optimum siting for a TDWR antennas would usually be some 8 - 12 miles from the runways.

Another TDWR is believed to serve Chicago Midway, about 15 miles from Chicago O'Hare. Obviously the sighting location is well inside maximum range of both radars and TDWR data would be interesting. But this not accessible on any public server, so far as can be ascertained.

NEXRAD

At least four WSR-88D antennas give overlapping coverage of the Chicago O'Hare region. The nearest at Romeoville, Ill. (*Fig.5*), is about 27 miles from Chicago O'Hare. The author acknowledges the help of James C. Smith in supplying detail images of the Romeoville NEXRAD weather product for four VCP 32 Clear Air Mode antenna scans bracketing the observation period. These are shown in *Fig.8* and *Fig.9* below.
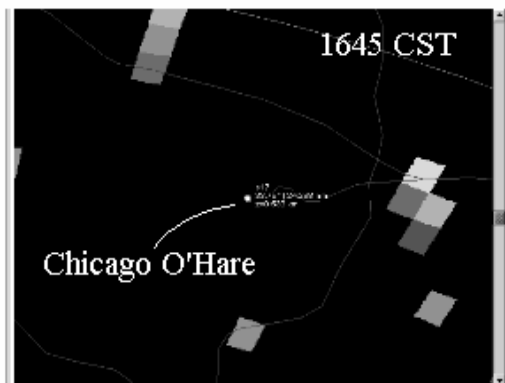
1635 CST

NEXRAD LEVEL-II
KLOT - CHICAGO, IL
11/07/2006 22:35:36 GMT
LAT: 41/36/17 N
LON: 88/05/05 W
ELEV: 663.0 FT
VCP: 32

REFLECTIVITY
ELEV ANGLE: 0.53
SCAN TIME: 22:35:35

O'Hare

radar

87.9102°W 41.9784°N (-2.0)
19.25° | 23.733 nmi
z=0.518 km

ground clutter

sun spike

Legend: (Category) dBZ

N/A
>= + 28
+ 24
+ 20
+ 16
+ 12
+ 8
+ 4
0
- 4
- 8
- 12
- 16
- 20
- 24
<= - 28

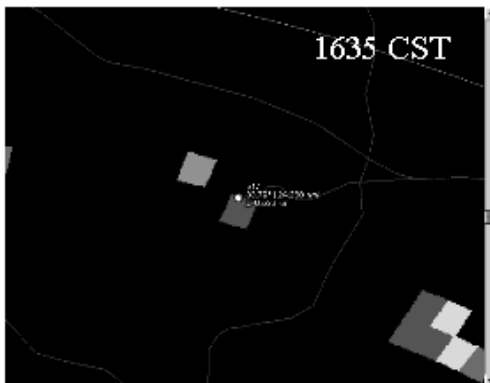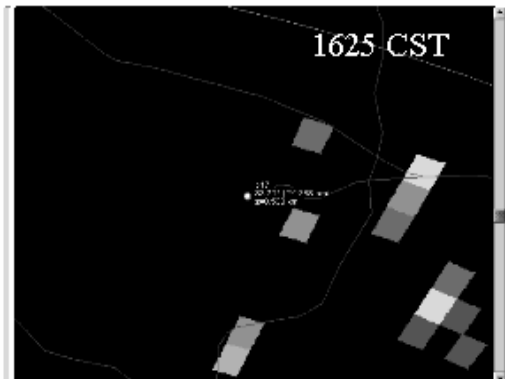1616 CST
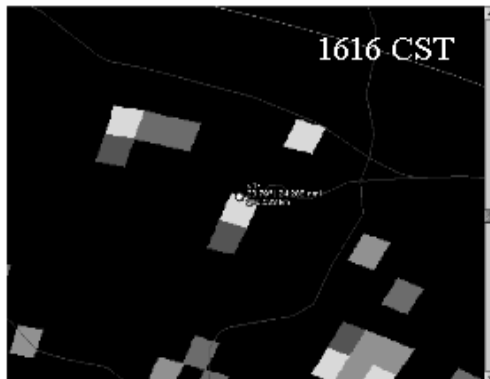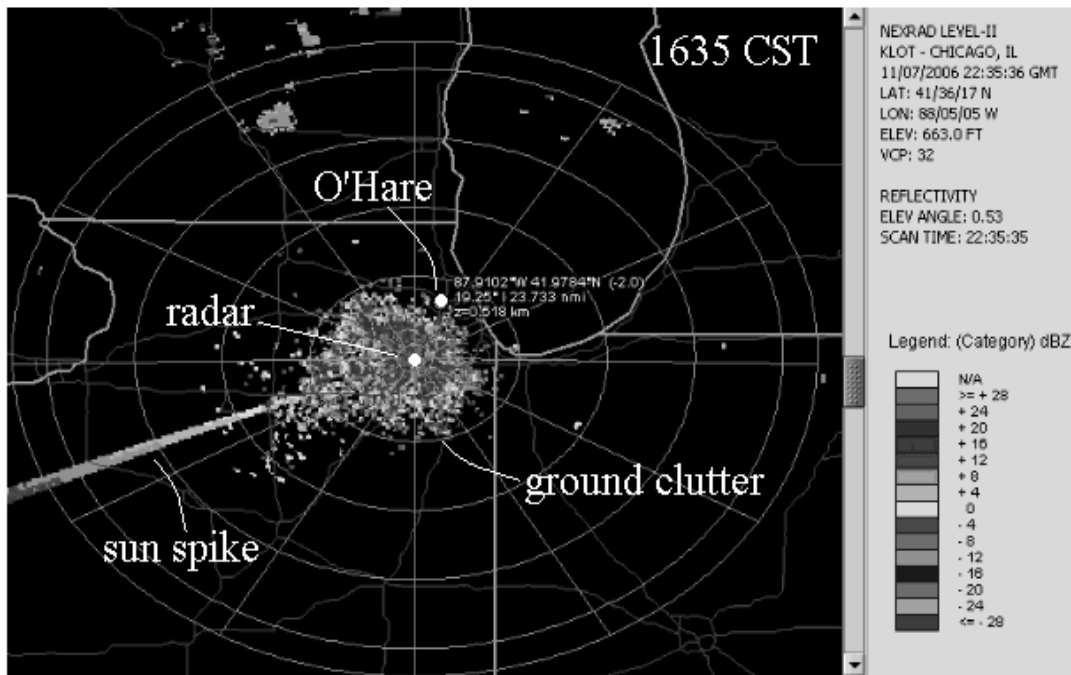
1625 CST

1635 CST

1645 CST

Chicago O'Hare

Fig.8 NEXRAD Base Reflectivity Radar Images Bracketing the
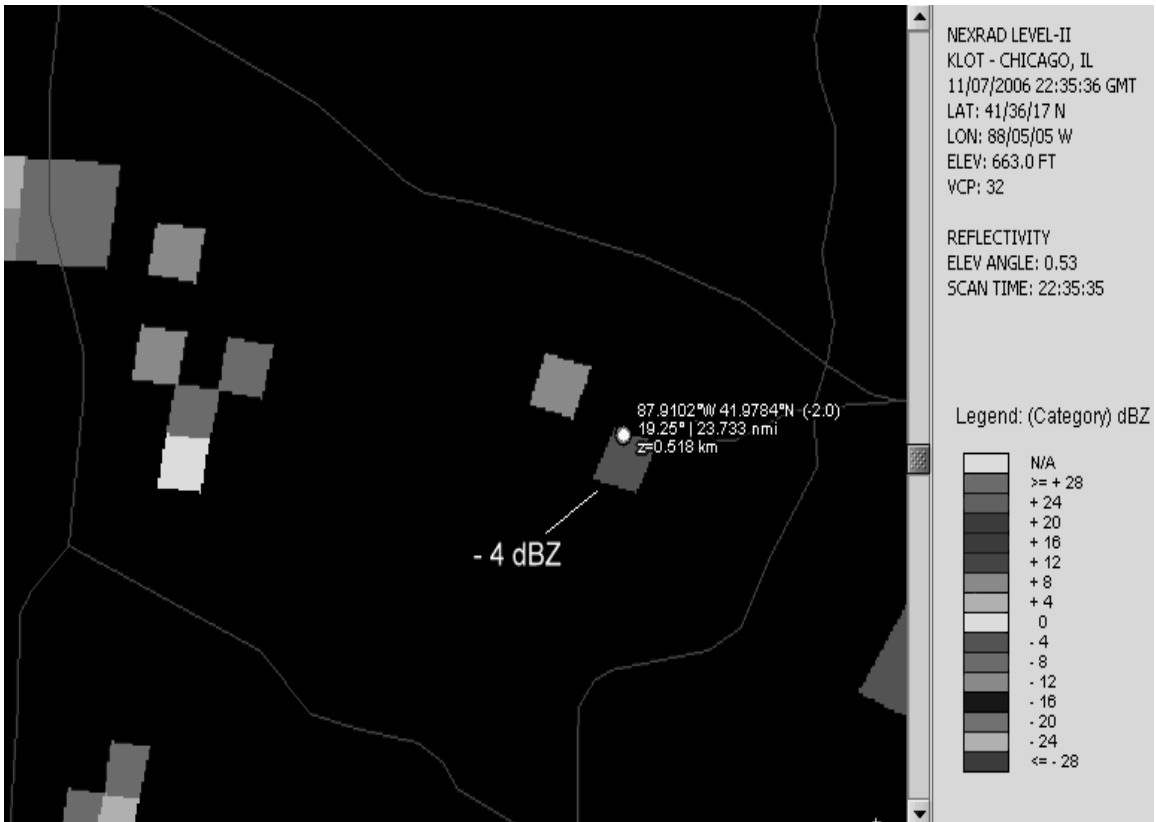Observation Period.

Fig 9 NEXRAD 0.5 degree Base Reflectivity Radar Image for 1635 CST
Showing echo detail over O'Hare Airport.

Fig 10 below shows the VCP 32 elevation coverage pattern of the radar. Complete volume coverage up to about 5 degrees is accompished in a number of scans of the ~1 degree beam at distinct elevations. The diagram shows that the full VCP 32 scan algorithm gives coverage at the range of the sighting location (27 nmi) up to an altitude of more than 15,000 ft. However for times around the sighting period only the lowest scan (0.53 deg) showed any data in the area of Chicago O'Hare, as shown in the images of the product from this scan in *Fig.8*
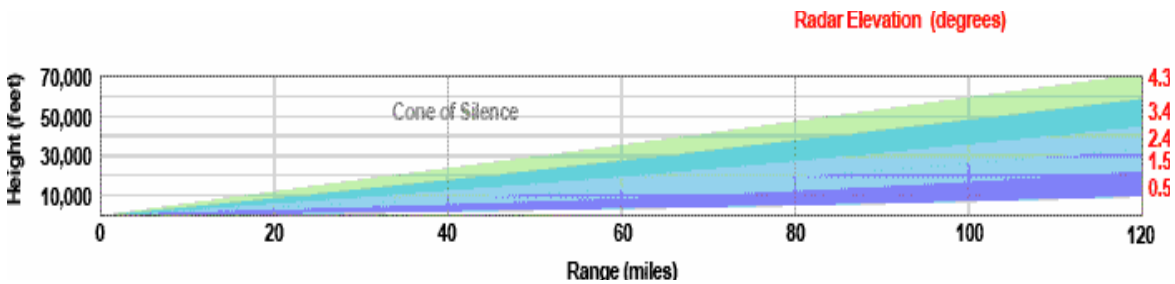

Fig.10. NEXRAD Volume Coverage Pattern VCP 31 & 32, Clear Air
Mode
(National Weather Service)

The images show that Romeoville WSR-88D did detect some echo, at an average signal reflectivity level less than light precipitation, in the resolution cell corresponding to the sighting location above Gate C-17 at 1616 CST, and again at 1635 CST, within a few minutes of the estimated sighting time.

Crudely speaking, a beam with a 1 degree cross-range resolution centered on a boresight elevation of 0.5 degrees covers an altitude to ~2300 ft at 24 nmi and the boresight is at ~ 1150 ft. However the reflectivity is averaged over a resolution cell whose ground footprint is so large (*Fig.11*) as to make this result of limited value.

Fig.11. Showing the footprint of the NEXRAD radar resolution cell
on the sighting location
(adapted from image supplied by James Smith)

Surface surveillance radar

ASDE-3

The ASDE-3 pencil beam is oriented so as to direct radar energy at negative elevations down towards the ground and little will be wasted at high elevations. Although aircraft landing and taking off can be detected, according to *Ref. 11*, "The ASDE-3 displays all vehicles that can be detected by primary surface radar out to about four nautical miles in range and up to approximately two hundred feet above ground level." These figures correspond to a positive top-edge elevation of approximately 0.5 deg. A target 1700 ft above Concourse C would be at nearly 20 degrees elevation even from the top of the tower. There seems to be little or no likelihood of relevant radar data from the ASDE-3.

5. Radar propagation conditions

Radar refractive index (RI) values were calculated for 32 elevated levels from 981 to 400 mbar using pressure, temperature and dewpoint readings from the 1800 CST Nov 7 2006 Davenport, Ill., rawinsonde balloon supplied in the NARCAP case #18 meteorology report (*ref.3*). The surface weather report for the balloon site provided surface readings, giving a total of 32 pairs of levels between the surface and ~24,000 ft. Each pair provides a gradient of refractive index in N-units per thousand feet, where $N = (n - 1) \times 10^6$, as shown in *Table 7*.

The standard atmosphere, corresponding to the "4/3 earth" refractivity model used in calculations in *Section 5*, is considered to have vertical gradient of -12 N/kft over land (a figure of 18 N/kft is usually adopted over water). This is the mean of a range between 0 and -24 N/kft taken to represent normal propagation; outside this range the atmosphere refracts radio energy in various ways that are generally regarded as "anomalous propagation".

Negative gradients steeper than -24 N/kft indicate superrefractive conditions, bending the radar beam earthwards more than normal; a gradient steeper than -48 N/kft is severely superrefractive, a trapping gradient; positive gradients - i.e., more than 0 N/kft - are subrefractive, bending the radar beam upward. Such features generally occur in relatively narrow layers of wide horizontal extent in a stable atmosphere, often but not exclusively developing during pre-dawn hours. A widespread "flat" pressure regime indicated by the general meteorological report (*ref.3*) suggests *conditions possibly favorable for widespread stratification in this case.*

pressure (mbar)	height (feet)	temp (°C)	dewpoint (°C)	R/I (N-units)	R/I gradient (N/kft)
1008.5	surface	11.1	6.7	320	
1000	235	—	—	—	0
981	751	10.8	6.4	320	-44
973	978	12.8	7.8	310	-14
925	2,375	10.0	6.6	300	-14
905	2,940	8.4	5.3	292	-51
904	2,999	8.5	4.8	289	-25
882	3,698	9.2	-0.8	272	-6
871	3,999	9.1	-1.8	270	-10
850	4,672	8.8	-3.2	259	-9
809	6,001	6.3	-7.3	252	-8
779	7,001	4.5	-10.4	240	-18
753	7,923	2.8	-13.2	223	-13
751	7,999	2.8	-16.3	222	-22
747	8,136	2.8	-22.2	219	-10
723	8,999	2.3	-27.8	210	-46
719	9,150	2.2	-28.8	203	-3
700	9,855	0.4	-27.6	201	-27
699	9,892	0.4	-25.6	200	+48
687	10,350	-0.5	-4.9	222	-14
670	11,000	-0.7	-8.0	213	-22
656	11,598	-0.9	-10.9	200	-17
645	12,001	-1.5	-14.3	193	-10
630	12,615	-2.5	-19.5	187	-11
597	13,999	-5.0	-17.6	179	+5
580	14,183	-5.3	-17.3	180	0
567	15,331	-7.9	-12.6	180	-7
552	16,000	-9.2	-14.8	175	-8
530	17,001	-11.1	-18.0	167	-17
500	18,504	-13.9	-22.9	156	-9
470	20,000	-17.6	-23.9	150	-8
451	21,000	-20.1	-24.5	142	-7
420	22,759	-24.5	-25.7	138	-8
400	23,917	-27.3	-28.8	131	

Table 7. Radar refractive index gradients in N-units per 1000 ft for 1800 CST Nov 7 (0000 GMT Nov 8) 2006, Davenport, Ill.

Of 32 gradients measured 25 were within the range of normal refractivity. Of 5 superrefractive pair gradients found, 2 are marginal (i.e., only one or two N-units outside the normal range) and 3 are significant. Of two subrefractive gradients, one is marginal (+5 N/kft) and one is significant.

The results from *Table 7* are graphed in the profile in *Fig.12*, showing the 4 significant gradients.
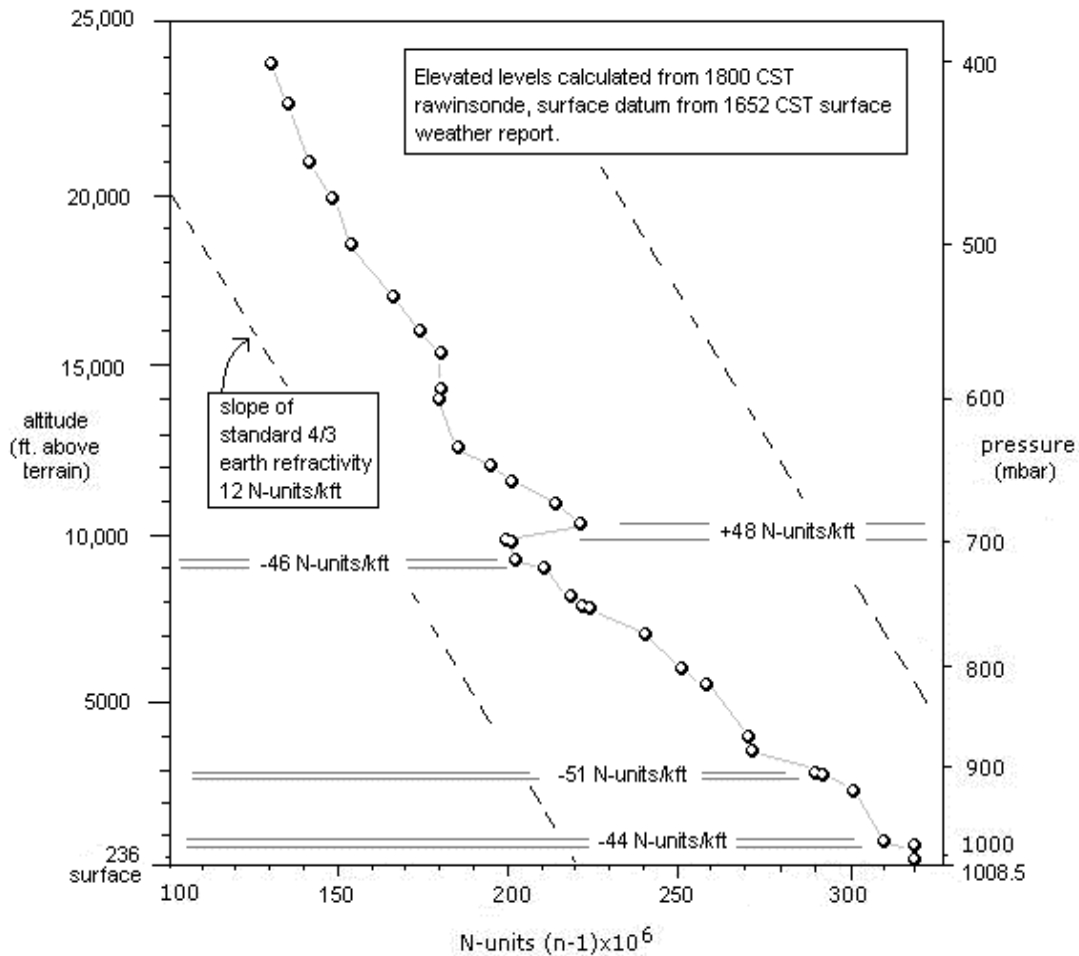

Fig.12. Radar refractivity profile for 1800 CST Nov 7 (0000 GMT Nov 8) 2006, Davenport, Ill., showing significant layers.

Through the first 750 ft the average RI gradient is zero; in other words rays traced through this region would (averaged) be straight lines instead of the 4/3 earth curves of normal propagation, a situation on the verge of becoming subrefractive. If representative of conditions through the depth of this surface layer, this suggests that the distance to the

radar horizon for energy emitted at low elevations will be somewhat reduced in radius, and the local area of permanent ground clutter would be somewhat reduced. This might enhance the subclutter visibility of targets at relatively short ranges from the radar.

Above this is a strongly superrefractive layer associated with a 2°C temperature inversion, the gradient then returning to normal above 1000 ft or so, until a narrow, sharp layer is encountered just below 3000 ft through which the RI drops by 51 N-units in about 60 ft of vertical ascent. This is a trapping gradient.

Radar energy entering this trapping layer can be refracted through an effective curve with a radius smaller than that of the Earth, returning to scatter off the surface some distance from the radar. If the layer is of large horizontal extent radar energy scattered back into the atmosphere from the surface after this process can be trapped a second time, and in this way a surface duct can be formed which may carry energy to large distances beyond the unambiguous range of the radar and return multiple-trip echoes by the same ray path. These echoes will display at arbitrary ranges on the PPI (the residual between some multiple of the unambiguous range and the true range to the remote reflector), but at the true azimuth of the reflector. Note however the staggered PRF technique employed by the ASR-9 radars, which should eliminate multiple-trip returns.

Around 9000 ft AGL there is another quite strongly superrefractive layer, and above that, passing through 10,000 ft, an unusual *sub*refractive layer with a strong positive gradient of +48 N/kft, associated with an overlying moist layer where relative humidity climbs from 12% to 72% through about 450 ft. Energy entering this layer will be refracted upwards, with the effect of reducing the radar horizon for some targets at higher elevations and leading heightfinder radars to underestimate altitudes for some targets above this layer.

Evidently there will be a general correlation between the severity of an RI gradient and the narrowness of the layer. Therefore, although there is no meteorological evidence of such, and although the highly stable unmixed air most favourable for extreme structures is least likely in the lower troposphere and in the late afternoon following solar warming, it is not possible to rule out the presence of sharper undetected gradients falling between the data points.

Research has indicated the possibility of gradients of 10^3 N-units per meter or more in certain conditions, which are capable of acting like radar mirrors. Such layers may have power reflection coefficients at low elevation angles capable of scattering significant energy to ground targets and back by near-specular partial reflection (efficiency inversely proportional to the 6th power of the cosecant of the elevation angle), and in some cases incoherent forward scatter from turbulent domains propagating across layer surfaces under the influence of winds are believed capable of generating discrete moving echoes in clear air. The reflection geometry is such that these echoes tend to move at twice the speed of the wind at the layer altitude, in the direction of the wind or at a moderate angle to the wind, and at twice the layer altitude, with the most favourable conditions occurring where there is a wind shear across the layer boundary causing turbulence in the shear zone.

In the present case, with winds veering 190-335 degs and climbing through 4 to 50 knots between the surface and 400 mbar, one would expect such echoes to move, in general, at an order of displayed speed between about 10 kts (low levels) and 100 kts (~24, 000 ft) with preferential headings varying between SW - NE and NW - SE respectively.

Of the three types of surveillance radars considered, only the ARSR-4 is capable of displaying primary height information and this radar has essentially no coverage of any of the levels below 24, 000 ft studied here. However by extrapolation from the winds aloft (rawinsonde readings are themselves only available up to about 30,000 ft) echoes from near-tropopausal layers (35,000 ft or more) on the ARSR-4 might be expected to show characteristic speeds of more than 200 knots on average headings between NW-SE or N-S.

There is no evidence of significant vertical velocity shear at any level where there is evidence of a significant RI gradient. The wind speed and direction changes across the four identified layers are shown in *Table 8*.

.

pressure level (mbar)	wnd speed (kts)	wnd direction (deg)
687	*17*	*315*
699	*16*	*317*
719	**16**	**305**
723	**16**	**307**
904	*6*	*263*
906	*6*	*265*
973	**4**	**190**
981	**4**	**198**

Table 8. Wind speed and direction for four pairs of levels having significant RI gradients

Low level temperature inversion layers can produce windshears by decoupling the momentum of winds above the inversion from surface friction forces on the winds below the inversion. Such shears can commonly reach tens of degrees of direction and tens of knots. In the present case part of the -44 N/kft refractive index gradient above 981 mbar (750 ft) is contributed by a small temperature inversion of 2°C. This is associated with an anticyclonic directional shear of only 8 degrees, and a speed shear of zero, through a layer of ~230 ft. Such a very weak shear would not be expected to cause turbulence of significance to the radar.

6. Conclusions

The NEXRAD weather radar data (*Section 4*) are not inconsistent with the presence of a radar-reflective target close to the 1900 ft cloud base within several minutes of the time of the visual report[2], but this is not probative evidence given the spatial size of the resolution cell, the slow update rate, and the distribution of stochastic echo evident in the several screenshots shown in *Fig. 8*.

Some comments on these factors are appropriate.

The radar was operating in mode VCP-32, which is one of two Clear Air modes usually used for routine monitoring in periods of quiet weather. The scan pattern (see *Fig.9*) takes over 10 minutes beginning with the low 0.5 deg cut. Two types of data are collected, the base reflectivity data (or simple echo intensity) and the doppler velocity data (measuring radial precipitation droplet velocity relative the the radar). The antenna then proceeds to scan several slices at higher elevations to build up the whole coverage volume. The data of interest here are for the 0.5 deg base reflectivity, obtained during the first 1-minute rotation of the scan pattern. (Neither the 0.5 deg doppler velocity product nor the higher cuts showed any data in the relevant area.)

The NEXRAD software generates automatic labels on the screen image. Referring to *Fig.12*, we can see that the elevation angle of the nominal 0.5 degree cut is actually 0.53 deg, and that the calculated height AGL of the beam at the relevant range $z = 0.518$ km, or about 1700 ft. This represents the boresight elevation, so the vertical coverage of the ~1 deg cross-range pencil beam will be from about 450 ft to 2950 ft. This will be calculated for a standard atmosphere, however, and given moderate superrefractivity (*Section 4*) these figures probably tend to overestimate the true heights. In any case, the reported object height clearly not only lies within the coverage zone but is quite close to the main gain. Note also that the WSR-88D employs horizontal linear polarisation to optimise reflectivity from the flattened lenticular profiles of falling water droplets. This would also tend to maximise echo from an object having the type of horizontal ellipsoidal

---

2 The the actual "scan time" is given as 22:35:36 UCT. If this is the time when the radar delivers the finished product from its complete volume scan, then it would indicate that the echo was collected 10 mins earlier, between about 16:25 and 16:26 CST, i.e., some 5 minutes prior to the approximate 16:31 time when visual sightings were made. If on the other hand this is the start time, or end time, of the initial 0.5 deg cut, then the echo was collected sometime between 16:34:36 and 16:36:36 CST, i.e., several minutes after the visual sighting time. The author has not found an authoritative answer to this, but it there is some internal evidence in favour of the second interpretation.

   This takes the form of a very interesting radial line at roughly 250 degs azimuth on the full area 16:35 image (*Fig.8*). This is very close to the azimuth of the sun which set at ~ 247.5 deg from the radar shortly after 16:43. It seems certain that this radial feature is a "sun spike" caused by solar EM energy radiated directly into the antenna. At 16:35 the sun was about 9 mins of arc above the optical horizon - corrected for normal refractivity - and allowing for the ~15% longer radar horizon could very plausibly have been close to the peak gain of a ~1 degree beam boresighted on 0.5 deg elevation. However 10 minutes earlier at 16:25 the sun was at 1 deg 53' elevation and thus more than two solar diameters away from the antenna boresight. This position would have been tens of dB down from the peak gain, so much less likely to produce a sun spike, and the direction of any correction due to superrefracted radar ray paths close to the horizon would be to increase this discrepancy. So tentatively we conclude that 16:35 CST +/- 1 minute is the true time of detection of this echo.

symmetry reported.

In this Clear Air mode the radar is extremely "alert" to faint echo (it automatically switches to a less sensitive Precipitation Mode when significant weather is detected). The reflectivity shown is an average over the whole resolution cell (*Fig.10*) and could be echo either from very weak sources dispersed over a large area, or from a localised region of much higher reflectivity somewhere inside that footprint. Surface weather reports state "no precipitation", and the 1635 echo is probably too faint for an area of precipitation anyway. However there is the possibility of transient surface clutter echoes. The splash of colour we see around the antenna in the small-scale area image is clearly ground clutter in this case. The echo we are interested in is not constant, i.e. doesn't appear on successive scans, so this might normally suggest it isn't ground echo. But it may be that AP conditions (for which there is evidence, see *Section 4*) fluctuate over time, allowing the radar to pick out faint ground echoes intermittently.

The radar can also image flocks of birds, or even insects and small airborne particulates, in addition to the summed reflectivity of one or more aircraft on approach or take-off that may be passing through that elevation slice at that time. The data block concerned (*Fig. 10*) seems to cover mostly apron and taxiways, but conceivably aircraft airborne at a few hundred feet near the SE and W ends respectively of runways 32L/14R or 9R/27L could be detected. Another conceivable source of intermittent faint echo in AP conditions might be airport buildings themselves, in particular the tall traffic control tower buildings. The ground-control tower appears to be within the radar cell footprint, although the new 250 ft AGL tower building falls just outside it.

In summary, the NEXRAD VCP-32 radar mode is very sensitive and there are several possible sources of faint echo. Echo is found in the relevant cell timed at 1635 CST. However each of the four scans investigated, sampling roughly 10% of the total coverage period between 1616 and 1645, shows a certain amount of intermittent echo of this type in the general area. In fact there is echo more than twice (~ 4dB) as strong in the same cell in the 1616 CST scan at a time when, apparently, no UFO was being seen. It can reasonably be argued that finding some echo within about a square km of the site within a few minutes of the sighting time is not too improbable. So whilst the height and location of the echo is not inconsistent with the presence of an object as reported, caution is recommended in drawing any conclusions.

If better data can be obtained, some factors to be borne in mind regarding radar coverage of the sighting area are:

- the range/altitude performance of radars may be modifed by the propagation conditions, differentially at low and high levels

- pulse Doppler MTD on all surveillance radars studied allows sub-clutter visibility of moving targets, but a stationary target might be rejected by the Doppler filters

- on the two ASR-9 radars (ORD#1, ORD #3) multiple-trip anomalous propagation echoes from beyond the unambiguous range caused by trapping conditions (see *Section 5*) should be filtered out by the staggered PRF technique employed

- the PPI display range scale selected may affect detectability - on the ASR-9 at minimum scale (60 nmi) the range to the reported object location from ORD #1 (0.78 nmi) is only 1.3 % of the PPI radius, or less than 3 mm from the geometric tube center on a 15" PPI, which may not be resolvable

- echo strength of close-in targets on the ASR-9 radars may also be artificially suppressed by the use of STC swept gain to suppress permanent clutter at the receiver/amplifier stage (see *Section 2*), which would affect the O'Hare ASR-9 (ORD #1) in particular. An attenuation of some 60 dB from the periphery to the centre of the scope may result with STC switched on, or a signal ratio of a million to one.

- the resolution cell (range discrimination x azimuth discrimination) of the O'Hare ASR-9 (ORD #1) at the range of the sighting location (Concourse C, Gate 17) is about 375 feet on the range axis by about 115 feet in azimuth.

- the resolution cell of the Oak Forest ASR-9 (ORD #3) at the range of the sighting location is about 375 feet on the range axis by about 3,230 feet in azimith

- the potential radar sample rate is limited by the rotation periods of the various radars. Considering the three surveillance radars (ASR-9s and ARSR-3) they collectively offer a possible 30 paints per minute, or 60-90 samples of the location during the reported sighting period of 2 - 3 mins.

- all surveillance sets studied have switchable polarisation, which might conceivably affect the signal returned by certain targets, i.e. circular polarisation might prejudice the detectability of resonators with a large degree of spherical symmetry

- other operational and human factors such as staffing, operator workload and vigilance etc., will affect the observation and reporting of any unidentified targets that are displayed - i.e., undeclared primary targets appearing at low level directly above the airport gates would be among the least anticipated potential hazards for air traffic controllers

References

1. *A Preliminary Design Process for Airspace Systems Initial Assessment - Chicago Case Study*, US Dept of Transportation report # VNTSC-DTS20-PDP-001.

2. *Air Traffic Control Factual Report*, National Transportation Safety Board, #DCA06MA009, May 24, 2006.

3. William Puckett, NARCAP Meteorology Consultant, *NARCAP Case #18 Meteorology Analysis*

4. Robert Sole, Brent L. Bedford, David Franc, and Timothy Pawlowitz, FAA report: *EFFECTS OF RF INTERFERENCE ON RADAR RECEIVERS*

5. D.A. Rhoda M.L. Pawlak. *Project Report NASA/A2, An Assessment of Thunderstorm Penetrations and Deviations by Commercial Aircraft in the Terminal Area*, 3 June, 1999

6. Leonard H Baker, *Fixed Ground Antenna Radome Operational Test and Evaluation*, DOT/FAA/CT-TN96/18 May 1996.

7. Mark E. Weber, *FAA SURVEILLANCE RADAR DATA AS A COMPLEMENT TO THE WSR-88D NETWORK* Massachusetts Institute of Technology, Lincoln Laboratory, Lexington, MA 02420-9185

8. Michael J. Istok and Peter Pickard, National Weather Service, Office of Science and Technology, Silver Spring, MD; Richard Okulski, National Weather Service, Office of Climate, Weather, and Water Services, Silver Spring, MD; Robert E. Saffle, Mitretek Systems, Inc., Falls Church, VA; Bill Bumgarner, BAE Systems, Washington, DC, *NWS Use of FAA Radar Data*

9. Mark A. Isaminger and Erik A. Proseus, *ANALYSIS OF THE INTEGRATED TERMINAL WEATHER SYSTEM (ITWS) 5-NM PRODUCT SUITE* Massachusetts Institute of Technology, Lincoln Laboratory, Lexington, Massachusetts 02420-9185

10. Federal R&D Needs and Priorities for Multifunction Phased Array Radar, http://www.ofcm.gov/r25-mpar/pdf/02-ch2.pdf

11. Airport surface vehicle identification US Patent 5334982, http://www.patentstorm.us/patents/5334982.html

12. FAA National Airspace System Architecture, http://nas-architecture.faa.gov/nas/location/location_data.cfm?FID=35